

# Neutrino oscillations from warped flavor symmetry: predictions for long baseline experiments T2K, NOvA and DUNE

Pedro Pasquini <sup>1,2,\*</sup>, S. C. Chuliá,<sup>†</sup> and J. W. F. Valle <sup>2‡</sup>

<sup>1</sup> *Instituto de Física Gleb Wataghin - UNICAMP,  
13083-859, Campinas SP, Brazil and*

<sup>2</sup> *AHEP Group, Institut de Física Corpuscular –  
C.S.I.C./Universitat de València, Parc Científic de Paterna.  
C/Catedrático José Beltrán, 2 E-46980 Paterna (València) - SPAIN*

## Abstract

Here we study the pattern of neutrino oscillations emerging from a previously proposed warped model construction incorporating  $\Delta(27)$  flavor symmetry [1]. In addition to a complete description of fermion masses, the model predicts the lepton mixing matrix in terms of two parameters. The good measurement of  $\theta_{13}$  makes these two parameters nearly proportional, leading to an approximate one-parameter description of neutrino oscillations. There is a sharp fourfold degenerate correlation between  $\delta_{CP}$  and the atmospheric mixing angle  $\theta_{23}$ , so that maximal  $\theta_{23}$  also implies maximal leptonic CP violation. The predicted electron neutrino and anti-neutrino appearance probabilities indicate that the model should be tested at the T2K, NOvA and DUNE long baseline oscillation experiments.

---

\* pasquini@ifi.unicamp.br

† salcen@alumni.uv.es

‡ valle@ific.uv.es, URL: <http://astroparticles.es/>

## I. INTRODUCTION

The striking pattern of neutrino mass and mixing parameters [2], remarkably at odds with that characterizing the quark sector, suggests that it can hardly be expected to happen just by chance. By and large, in the attempt to bring a rationale to the pattern of fermion mixing, theorists have focused on the idea that there is some yet-to-be-determined non-Abelian flavor symmetry of nature. Theoretical work towards predicting flavor parameters has followed two complementary paths, namely:

- Building explicit flavor models on a case-by-case basis [3–7]
- Focussing upon the residual CP symmetries characterizing the final mass matrices, irrespective of the details of the underlying theory [8, 9]

In both cases a number of predictions for the leptonic mixing matrix can be made. Specially interesting for phenomenology are those which imply a correlation between the leptonic Jarlskog invariant

$$J_{CP} = \text{Im}[U_{e1}^* U_{\mu 3}^* U_{\mu 1} U_{e3}]$$

and the atmospheric angle, since  $\delta_{CP}$  and  $\theta_{23}$  are the two less precisely determined of all the neutrino oscillation parameters.

Despite enormous experimental effort since the discovery of neutrino oscillations [10, 11], we are still far from a high precision measurement of the leptonic CP phase characterizing neutrino oscillations within the three flavor paradigm [12]. In this paper we focus on a model where neutrino oscillations are, to a good approximation, described in terms of a unique parameter that may be taken as  $\delta_{CP}$ .

For definiteness, we focus upon symmetry based flavor models. We consider the case of a full-fledged warped model construction incorporating flavor symmetry [1]. It provides an explicit proof-of-concept, realizing a realistic and “natural” scheme providing a complete description of all fermion masses as well as their mixing angles and phases. All mass hierarchies are naturally accounted for by warping. Thanks to the underlying  $\Delta(27)$  flavor symmetry, the model implies a predictive pattern of lepton mixing parameters, while adequately fitting the quark mixing matrix. Here we determine the implications of the model for neutrino oscillations, deriving the manifest correlation between  $\delta_{CP}$  and the atmospheric angle  $\theta_{23}$ . We find that the determination of leptonic CP violation is no longer unique but exhibits a fourfold degeneracy. This is used to work out the predicted electron neutrino and anti-neutrino appearance probabilities for the long baseline neutrino oscillation experiments T2K, NOvA and the upcoming DUNE [13] experiment.

## II. THEORY PRELIMINARIES: THE WARPED FLAVOR MODEL

Here the main idea consists in combining the advantages of warping in order to account for mass hierarchies without fine tuning, with those of implementing flavor symmetries, in order to potentially predict the fermion mixing pattern. For definiteness we focus on the Warped Flavor Model proposed in [1]. The model is a minimal version of the Randall-Sundrum (RS) model involving compactification of the fifth dimension on  $S_1/\mathbb{Z}_2$  and attaching the orbifold to  $y = 0$  (UV brane) and  $y = L$  (IR brane). The warped five-dimensional  $AdS_5$  metric is given as

$$ds^2 = e^{-2ky} \eta_{\mu\nu} dx^\mu dx^\nu - dy^2, \quad (1)$$

where  $\eta_{\mu\nu} = \text{Diag}[1, -1 - 1 - 1]$  and  $k$  is the curvature scale parameter.

We employ the most minimal version of the RS model with non-custodial  $G_{\text{SM}} = SU(2)_L \otimes U(1)_Y$  bulk electroweak symmetry where the 5D fermions and the Higgs field,  $H$ , are allowed to propagate into the bulk. Although models with a brane-localized Higgs and no custodial symmetry are severely constrained by electroweak precision tests [14] the conflict with electroweak and flavour physics constraints can be significantly reduced when the 5D Higgs field lives in the bulk [15–20]. This offers a way to account for fermion mass hierarchies while evading electroweak and flavour physics restrictions. Besides the usual SM states, 4 extra scalars are added to the model,  $\phi, \sigma_1, \sigma_2$  and  $\xi$ , all of which acquire vacuum expectation values. It has been shown that charged lepton as well as Dirac neutrino masses are generated at leading order [1]. Moreover, all fermion mass hierarchies can be adequately described by appropriate choices of bulk mass parameters [1]. On the other hand *Dirac* neutrino masses are generated by interactions in the IR brane of the form  $\sim (\xi \sigma_a \bar{\Psi}_l) \tilde{H} \Psi_{\nu_i}$ . As a result, the double vev of the scalars and the localization of the interaction can naturally account for their smallness.

Concerning the mixing angles, a beautiful feature of the model consists in the integration of its extra-dimensional nature with the implementation of a non-Abelian flavor symmetry, in our case  $\Delta(27) \otimes \mathcal{Z}_4 \otimes \mathcal{Z}'_4$ . The latter leads to the prediction of all the 4 neutrino oscillation parameters in terms of just two angles:  $\theta_\nu$  and  $\phi_\nu$  according to the following equations,

$$\sin^2 \theta_{12} = \frac{1}{2 - \sin 2\theta_\nu \cos \phi_\nu} \quad (2)$$

$$\sin^2 \theta_{13} = \frac{1}{3} (1 + \sin 2\theta_\nu \cos \phi_\nu) \quad (3)$$

$$\sin^2 \theta_{23} = \frac{1 - \sin 2\theta_\nu \sin(\pi/6 - \phi_\nu)}{2 - \sin 2\theta_\nu \cos \phi_\nu} \quad (4)$$

$$J_{\text{CP}} = -\frac{1}{6\sqrt{3}} \cos 2\theta_\nu, \quad (5)$$

where  $J_{\text{CP}}$  is the Jarlskog invariant.

These relations were derived in [1] and they imply that the theory can be directly probed using low energy neutrino oscillation experiments by comparing the above predicted relations, given in terms of the two free parameters  $\theta_\nu$  and  $\phi_\nu$ , with the measured oscillation parameters. Indeed, the allowed parameter region consistent with current oscillation data [12] can be determined and was given in [1]. Here we refine and extend the analysis so as to isolate the implications of the model. In Fig. 1 we present the  $3\sigma$  and  $2\sigma$  regions of model parameters allowed by the current neutrino oscillation global fit in [12].

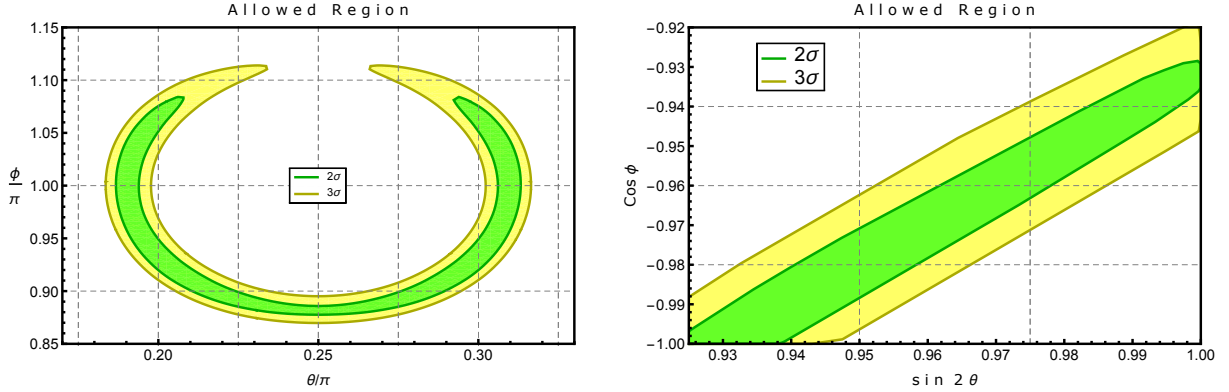


FIG. 1. Two ways of displaying the  $3\sigma$  (yellow) and  $2\sigma$  (green) regions of model parameters  $\theta_\nu$  and  $\phi_\nu$  allowed by global fit of current neutrino oscillation data.

In the left panel of this figure we show the  $3\sigma$  and  $2\sigma$  allowed contours obtained using the global  $\chi^2$  function,

$$\chi_{\text{Global}}^2 = \chi_{12}^2 + \chi_{13}^2 + \chi_{23}^2, \quad (6)$$

where in  $\chi_{1i}^2$  we assumed Gaussian prior corresponding to the global fit determinations of  $\sin^2 \theta_{12}$  and  $\sin^2 \theta_{13}$ ,

$$\chi_{1i}^2 = \left( \frac{\sin^2 \theta_{1i}^{\text{exp}} - \sin^2 \theta_{1i}^{\text{pred}}}{\sigma_{1i}} \right)^2 \quad (7)$$

for  $i = 2, 3$ , the  $\sigma_{1i}$  the Gaussian error at  $1\sigma$ , while the  $\chi_{23}^2$  is the function for  $\sin^2 \theta_{23}$  used in [12]. Following [1], the predicted values for the mixing angles  $\theta_{ij}$  are calculated by varying  $\theta_\nu$  and  $\phi_\nu$  given in Eqs. 2-4 <sup>1</sup>, leading to the regions depicted in the left panel in Fig. 1. In the right panel we highlight the effect of the precise determination of the reactor mixing angle  $\theta_{13}$  at Daya Bay. Indeed, from Eq. 3 it follows that the two model parameters  $\theta_\nu$  and  $\phi_\nu$  are sharply correlated, as displayed in the figure. Hence, in an approximate sense our model is an effectively one parameter model for neutrino oscillations.

<sup>1</sup> Note however that, instead of taking the individual  $\chi^2$  as in [1], here we add them up, resulting in a slightly more restrictive constraint, as expected.

The Global  $\chi^2$ -analysis has two minima  $\chi_{\min}^2 = 3.81$  found for: (1)  $\theta_\nu^1 = 0.295\pi$  and  $\phi_\nu = 0.92\pi$  and (2)  $\theta_\nu^2 = 0.205\pi$  and  $\phi_\nu = 0.92\pi$  corresponding to the mixing parameters given in Table I. This degeneracy is trigonometric, as  $\theta_\nu^i$  are complementary, that is,  $\theta_\nu^1 + \theta_\nu^2 = 90^\circ$  and Eqs. 2-4 contain only  $\sin 2\theta_\nu$ . However this degeneracy is lifted by a measurement of the Jarlskog invariant. The latter is proportional to  $\cos 2\theta_\nu$  and, by itself, gives rise to a fourfold degeneracy in  $\delta_{\text{CP}}$  as can be seen in Fig.3. Together with the neutrino oscillation data determining the mixing angles one finds a solution  $\delta_{\text{CP}} = 1.27\pi$  deeper than the other minima, as presented in Fig.2.

Parameter	Minimum 1	Minimum 2	Unconstrained case
$s_{12}^2$	0.341	0.341	0.323( $\pm 0.016$ )
$s_{13}^2$	0.0232	0.0232	0.0234( $\pm 0.0020$ )
$s_{23}^2$	0.570	0.570	0.573( $^{+0.025}_{-0.043}$ )
$\delta_{\text{CP}}/\pi$	1.27(1.72)	0.72(0.27)	1.34( $^{+0.64}_{-0.38}$ )

TABLE I. Predicted values of the neutrino oscillation parameters  $s_{ij}^2 = \sin^2 \theta_{ij}$  corresponding to the  $\chi^2$  minima obtained in our model for different  $(\theta_\nu, \phi_\nu)$  values. The fourth column denotes the standard “unconstrained” three-neutrino best fit values from [12].

One notices that the preferred value of  $\delta_{\text{CP}}$  in our model can be quite different from that found in the general “unconstrained” three-neutrino oscillation scenario. To see this closer we plot in Fig. 2 the  $\Delta\chi^2$  function assuming our model to be true and compare with what is found in the general “unconstrained” three-neutrino oscillation global fit. The solid black curve gives the total  $\Delta\chi^2$  in our model as  $\chi_{\text{Total}}^2 = \chi_{\text{Global}}^2 + \chi_\delta^2$ , while the black-dashed one corresponds to the “unconstrained”  $\chi_\delta^2$  function in [12]. One notices that there are four nearly degenerate preferred minima of  $\delta_{\text{CP}}$  in our model, all allowed at  $2\sigma$ . These minima are narrower than the unique determination of  $\delta_{\text{CP}}$  found in the general “unconstrained” case. By providing an improved determination of  $\delta_{\text{CP}}$ , future data could make the difference between our model and the general case potentially significant. Namely, within our model  $\delta_{\text{CP}}$  has a more precisely determined value than in the general case.

In addition, an improved  $\delta_{\text{CP}}$  determination would also imply a determination of the atmospheric mixing angle  $\theta_{23}$  in our model, as seen in Fig. 3 below. Indeed our model predicts a sharp correlation between  $\delta_{\text{CP}}$  and  $\theta_{23}$  as illustrated in Fig.3. As one can see, a feature of this predicted correlation is that maximal mixing  $\theta_{23} = \pi/4$  also implies maximal CP violation (up to sign), a remarkable prediction indeed.

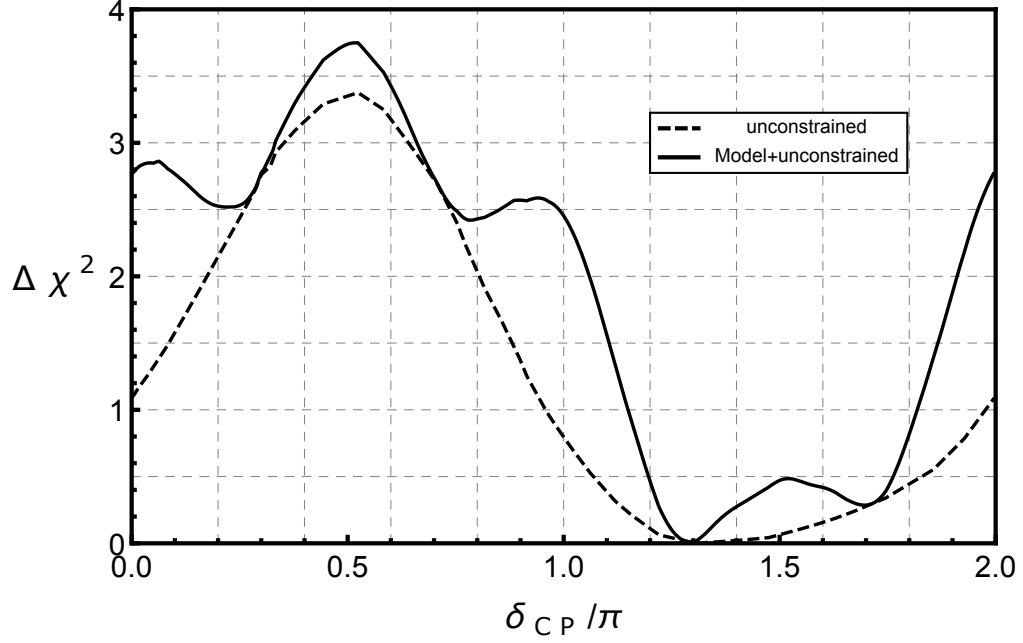


FIG. 2.  $\Delta\chi^2$  as a function of  $\delta_{\text{CP}}$  for our model (solid line) and for the general case (dashed line).

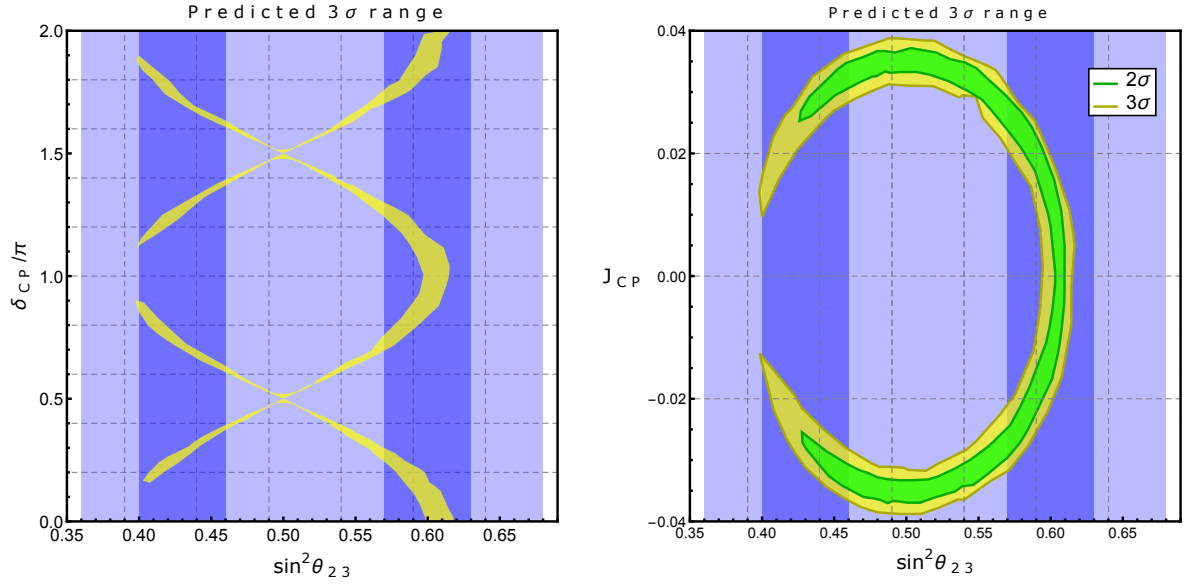


FIG. 3. Values of leptonic CP violation parameter allowed by current oscillation data versus the atmospheric angle  $\theta_{23}$ . Vertical bands are allowed at  $3\sigma$  (light blue) and  $1\sigma$  (darker blue) by the global fit in [12]. **Left:** The yellow region denotes the  $3\sigma$  region of  $\delta_{\text{CP}}$ . **Right:** The yellow and green regions denote the  $3\sigma$  and  $2\sigma$  regions of  $J_{\text{CP}}$ , the Jarlskog invariant.

### III. PREDICTIONS FOR THE T2K, NOVA AND DUNE EXPERIMENTS

As we saw above, the fact that the model contains only two tightly correlated free parameters suggests that it will be tested in future long baseline neutrino oscillation experiments. In order to see the effect of the restricted neutrino oscillation parameter space we have mapped out the resulting allowed values for the oscillation probability and compared with those expected in a generic model. To do this we varied the parameters  $\theta_\nu$  and  $\phi_\nu$  inside the  $3\sigma$  range of Fig. 1 (Left). Of special interest here are those experiments that can probe the parameter  $\delta_{\text{CP}}$  (or  $\theta_{13}$ ), as these play a key role to constrain our parameter space. Indeed, any of these can be taken as “the” key parameter of our model.

The presence of CP violation in long baseline accelerator neutrino oscillation experiments would be manifest in the most direct way through the non-vanishing of the neutrino oscillation CP asymmetry  $A_{\mu e} = (P_{\mu e} - P_{\bar{\mu} \bar{e}})/(P_{\mu e} + P_{\bar{\mu} \bar{e}})$ . However here we prefer to display the individual neutrino and antineutrino oscillation probabilities, as these contain all the information. Matter effects are included in our calculations according to Ref. [21].

In the left panel in Fig. 4 we show the allowed regions of the oscillation probability expected within the generic three-neutrino oscillation scheme, as a function of the detector distance for a 1 GeV neutrino. The large spread in the allowed region for the appearance probabilities follows mainly from our poor knowledge of the  $\delta_{\text{CP}}$  phase.

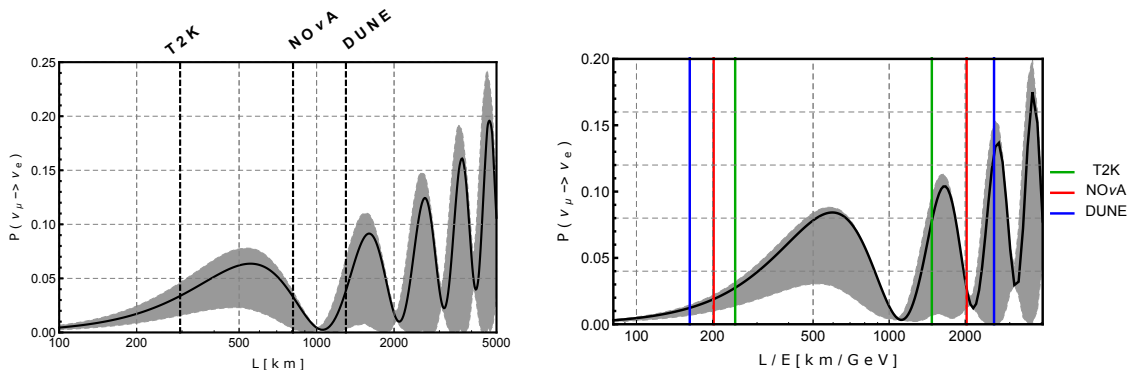


FIG. 4. **Left:** Transition probability  $P(\mu \rightarrow e)$  as a function of the distance,  $L$ , of the detector for a 1 GeV neutrino expected in the generic three-neutrino oscillation scheme. The shaded region represents the  $3\sigma$  range while the solid line corresponds to the current best fit. Vertical lines indicate the T2K, NOvA and DUNE baselines. **Right:** The probability as a function of  $L/E$ , the color vertical lines indicating the  $L/E$  ranges covered in each experiment.

In order to get a closer look on our model predictions compared to the general unconstrained case we display the neutrino oscillation probabilities expected in each experiment. These are plotted in Figs. 5-8 for T2K, NOvA and DUNE respectively. The gray area corresponds to the case of no model constraints, while the color regions correspond to the

predictions of our model. The solid line represents the unconstrained  $\chi^2$  minimum in each case with  $\delta_{CP} = 3\pi/2$ , while the dashed and dotted lines correspond to minimum 1 and minimum 2 respectively, see Table. In Figs. 5 and 6 the left panel gives the neutrino and the right one the anti-neutrino transition probabilities. Fig. 7 shows the same transition probability for neutrinos as a function of the energy in the left and as a function of the distance in the right, while Fig. 8 shows the same for antineutrinos.

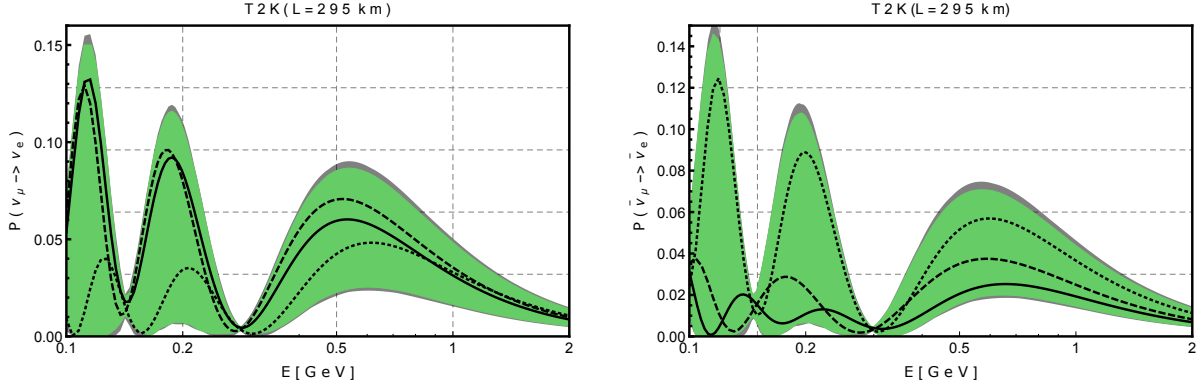


FIG. 5. Transition probability as a function of the neutrino energy,  $E$ , for the T2K experiment. The green area represents the  $3\sigma$  allowed region in the model while the gray one represents the  $3\sigma$  allowed region in the unconstrained case. The full line represents the current neutrino best fit with  $\delta_{CP} = 3\pi/2$ , the dashed line is the minimum 1 for  $\delta_{CP} = 1.27\pi$  and the dotted line the minimum 2 for  $\delta_{CP} = 0.27\pi$ . **Left:**  $P(\mu \rightarrow e)$  transition probability. **Right:**  $P(\bar{\mu} \rightarrow \bar{e})$  transition probability.

From Figs. 5 and 6 one sees that the currently allowed  $3\sigma$  ranges for the oscillation probabilities are only slightly wider for the generic or “unconstrained” model than for our case, characterizing the good measurement of the mixing angles. The predictivity of our model consists mainly in the fourfold correlation depicted in the left panel in Fig. 3. The large difference between the dashed and dotted curves comes from the large difference in the  $\delta_{CP}$  values associated to the minima in the Table which, in turn, are associated to the fourfold degeneracy. Indeed, as can be seen in Fig. 2, these minima can have  $\delta_{CP}$  values very different from the current preferred one, especially in the first oscillation peaks.

We now turn to the predictions for neutrino and anti-neutrino oscillation probabilities for the case of the DUNE experiment, with baseline 1300 km. In this case matter effects play a more important role than in the previous ones. As before we will take, for illustration, the deeper global minimum in Fig. 2 (Minimum 1 with  $\delta_{CP} = 1.27\pi$ ) as the true one and compare it with Minimum 2 corresponding to  $\delta_{CP} = 0.27\pi$  and with the “standard” case with  $\delta_{CP} = 3\pi/2$ .

In Fig. 7 we show  $\mu \rightarrow e$  the transition probability for DUNE as a function of the



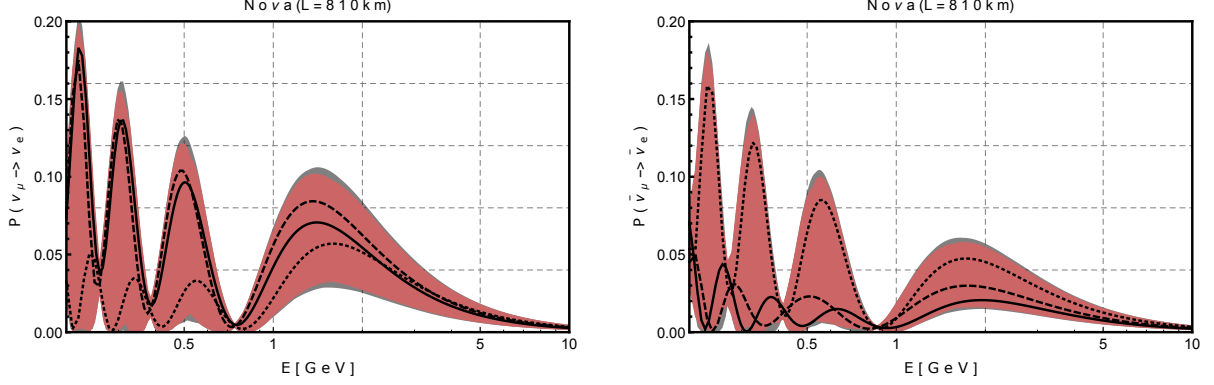


FIG. 6. Transition probability as a function of the neutrino energy,  $E$ , for the *Nova* experiment. The red area represents the  $3\sigma$  allowed region in the model while the gray one represents the  $3\sigma$  allowed region in the unconstrained case. The full line represents the current neutrino best fit with  $\delta_{CP} = 3\pi/2$ , the dashed line is the minimum 1 for  $\delta_{CP} = 1.27\pi$  and the dotted line the minimum 2 for  $\delta_{CP} = 0.27\pi$ . **Left:**  $P(\mu \rightarrow e)$  transition probability. **Right:**  $P(\bar{\mu} \rightarrow \bar{e})$  transition probability.

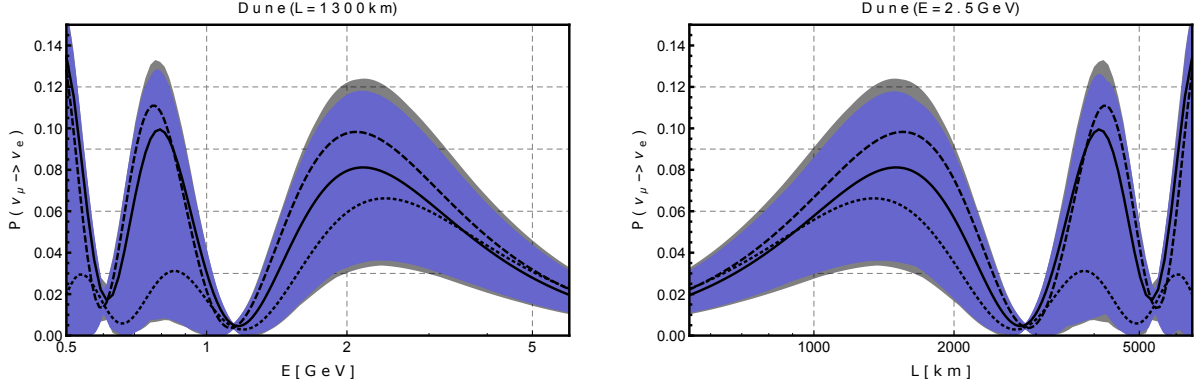


FIG. 7. **Left:** Transition probability as a function of the neutrino energy,  $E$ , for the DUNE experiment. **Right:**  $P(\mu \rightarrow e)$  as a function of the baseline  $L$  for the energy peak at  $E = 2.5$  GeV. The solid line represents the current neutrino best fit with  $\delta_{CP} = 3\pi/2$ , while the dashed and dotted lines correspond to minima with  $\delta_{CP} = 1.27\pi$  and with  $\delta_{CP} = 0.27\pi$ , respectively.

neutrino energy,  $E$ . In the right panel we display the oscillation probability as a function of the baseline  $L$  for peak energy at  $E = 2.5$  GeV. The solid line corresponds to the current neutrino best fit with  $\delta_{CP} = 3\pi/2$ , while the dashed and dotted ones correspond to the minima with  $\delta_{CP} = 1.27\pi$  and  $\delta_{CP} = 0.27\pi$ , respectively. As an example one sees how the model allows for a potentially large shift in the position of the first oscillation maximum as well as its height, as seen in the expected shape of the transition probabilities, making the

model potentially testable.

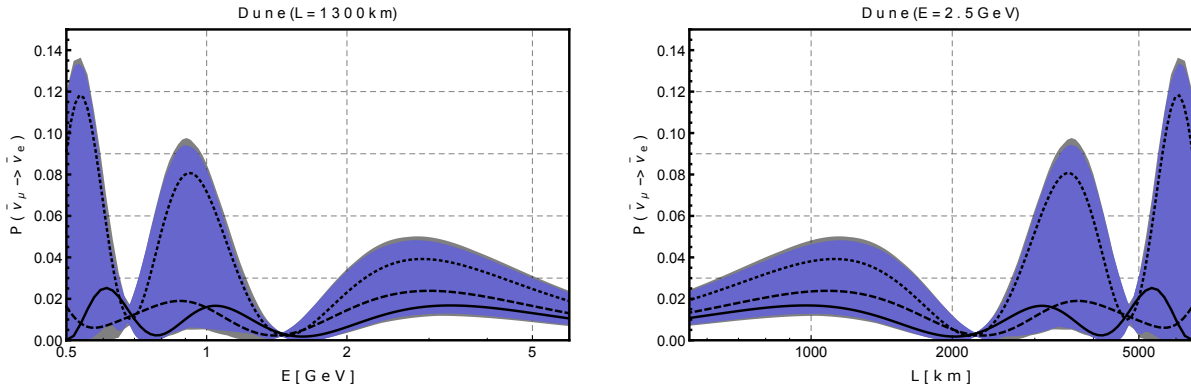


FIG. 8. Same as Fig. 7, but for the  $\bar{\mu} \rightarrow \bar{e}$  oscillation probability.

#### IV. DISCUSSION AND CONCLUSION

We have characterized neutrino oscillation predictions emerging from a previously proposed warped model construction incorporating  $\Delta(27)$  flavor symmetry [1]. Fermion masses and mixing are all accommodated in a realistic way, while the pattern of neutrino oscillations is described in terms of two parameters  $\cos \phi_\nu$  and  $\sin 2\theta_\nu$  nearly proportional to each other. The determination of  $\delta_{CP}$  is fourfold degenerate with the minima allowed within  $2\sigma$ , as seen in Fig. 2. The sharp correlation between  $\delta_{CP}$  and the atmospheric mixing angle  $\theta_{23}$  seen in Fig. 3 encodes the true predictive power of the model, and implies that maximal  $\theta_{23}$  is associated with maximal leptonic CP violation. We have seen how there can be substantial differences in the appearance neutrino and anti-neutrino probabilities for the long baseline accelerator experiments. Our results for the T2K, NO $\nu$ A and DUNE experiments suggest that the model should potentially be put to a stringent test. Indeed these experiments could, in principle, rule it out, especially after improved determinations of  $\delta_{CP}$  and the  $\theta_{23}$  octant.

#### V. ACKNOWLEDGEMENTS

Work supported by Spanish grants FPA2014-58183-P, Multidark CSD2009-00064, SEV-2014-0398 (MINECO) and PROMETEOII/2014/084 (Generalitat Valenciana). P. S. P.

acknowledges the support of FAPESP grant 2014/05133-1, 2015/16809-9 and 2014/19164-6.

- 
- [1] P. Chen, G.-J. Ding, A. D. Rojas, C. A. Vaquera-Araujo, and J. W. F. Valle, “Warped flavor symmetry predictions for neutrino physics,” *JHEP* **01** (2016) 007, [arXiv:1509.06683 \[hep-ph\]](#).
  - [2] **Particle Data Group** Collaboration, K. A. Olive *et al.*, “Review of Particle Physics,” *Chin. Phys.* **C38** (2014) 090001.
  - [3] K. S. Babu, E. Ma, and J. W. F. Valle, “Underlying  $a(4)$  symmetry for the neutrino mass matrix and the quark mixing matrix,” *Phys. Lett.* **B552** (2003) 207–213, [hep-ph/0206292](#).
  - [4] G. Altarelli and F. Feruglio, “Discrete Flavor Symmetries and Models of Neutrino Mixing,” *Rev.Mod.Phys.* **82** (2010) 2701–2729, [arXiv:1002.0211 \[hep-ph\]](#).
  - [5] S. Morisi and J. W. F. Valle, “Neutrino masses and mixing: a flavour symmetry roadmap,” *Fortsch.Phys.* **61** (2013) 466–492, [arXiv:1206.6678 \[hep-ph\]](#).
  - [6] S. Morisi, D. Forero, J. C. Romao, and J. W. F. Valle, “Neutrino mixing with revamped  $A_4$  flavour symmetry,” *Phys.Rev.* **D88** (2013) 016003, [arXiv:1305.6774 \[hep-ph\]](#).
  - [7] S. F. King, A. Merle, S. Morisi, Y. Shimizu, and M. Tanimoto, “Neutrino Mass and Mixing: from Theory to Experiment,” *New J.Phys.* **16** (2014) 045018, [arXiv:1402.4271 \[hep-ph\]](#).
  - [8] P. Chen, G.-J. Ding, F. Gonzalez-Canales, and J. W. F. Valle, “Generalized  $\mu - \tau$  reflection symmetry and leptonic CP violation,” *Phys. Lett.* **B753** (2016) 644–652, [arXiv:1512.01551 \[hep-ph\]](#).
  - [9] P. Chen, G.-J. Ding, F. Gonzalez-Canales, and J. W. F. Valle, “Classifying CP transformations according to their texture zeros: theory and implications,” *Phys. Rev.* **D94** no. 3, (2016) 033002, [arXiv:1604.03510 \[hep-ph\]](#).
  - [10] T. Kajita, “Nobel Lecture: Discovery of atmospheric neutrino oscillations,” *Rev. Mod. Phys.* **88** no. 3, (2016) 030501.
  - [11] A. B. McDonald, “Nobel Lecture: The Sudbury Neutrino Observatory: Observation of flavor change for solar neutrinos,” *Rev. Mod. Phys.* **88** no. 3, (2016) 030502.
  - [12] D. V. Forero, M. Tortola, and J. W. F. Valle, “Neutrino oscillations refitted,” *Phys. Rev.* **D90** no. 9, (2014) 093006, [arXiv:1405.7540 \[hep-ph\]](#).
  - [13] **DUNE** Collaboration, R. Acciarri *et al.*, “Long-Baseline Neutrino Facility (LBNF) and Deep Underground Neutrino Experiment (DUNE),” [arXiv:1512.06148 \[physics.ins-det\]](#).
  - [14] C. Csaki, J. Erlich, and J. Terning, “The Effective Lagrangian in the Randall-Sundrum model and electroweak physics,” *Phys. Rev.* **D66** (2002) 064021, [arXiv:hep-ph/0203034 \[hep-ph\]](#).
  - [15] J. A. Cabrer, G. von Gersdorff, and M. Quiros, “Suppressing Electroweak Precision Observables in 5D Warped Models,” *JHEP* **05** (2011) 083, [arXiv:1103.1388 \[hep-ph\]](#).

- [16] A. Carmona, E. Ponton, and J. Santiago, “Phenomenology of Non-Custodial Warped Models,” *JHEP* **10** (2011) 137, [arXiv:1107.1500 \[hep-ph\]](#).
- [17] P. R. Archer, M. Carena, A. Carmona, and M. Neubert, “Higgs Production and Decay in Models of a Warped Extra Dimension with a Bulk Higgs,” *JHEP* **01** (2015) 060, [arXiv:1408.5406 \[hep-ph\]](#).
- [18] K. Agashe, A. Azatov, and L. Zhu, “Flavor Violation Tests of Warped/Composite SM in the Two-Site Approach,” *Phys. Rev.* **D79** (2009) 056006, [arXiv:0810.1016 \[hep-ph\]](#).
- [19] P. R. Archer, S. J. Huber, and S. Jager, “Flavour Physics in the Soft Wall Model,” *JHEP* **12** (2011) 101, [arXiv:1108.1433 \[hep-ph\]](#).
- [20] J. A. Cabrer, G. von Gersdorff, and M. Quiros, “Flavor Phenomenology in General 5D Warped Spaces,” *JHEP* **01** (2012) 033, [arXiv:1110.3324 \[hep-ph\]](#).
- [21] H. Nunokawa, S. Parke, and J. W. Valle, “{CP} violation and neutrino oscillations,” *Progress in Particle and Nuclear Physics* **60** no. 2, (2008) 338 – 402.  
<http://www.sciencedirect.com/science/article/pii/S014664100700083X>.